AIP Journal of Applied Physics

Electron-beam irradiation-induced gate oxide degradation

Byung Jin Cho, Pei Fen Chong, Eng Fong Chor, Moon Sig Joo, and In Seok Yeo

Citation: J. Appl. Phys. 88, 6731 (2000); doi: 10.1063/1.1321030
View online: http://dx.doi.org/10.1063/1.1321030
View Table of Contents: http://jap.aip.org/resource/1/JAPIAU/v88/i11
Published by the American Institute of Physics.

Additional information on J. Appl. Phys.

Journal Homepage: http://jap.aip.org/
Journal Information: http://jap.aip.org/about/about_the_journal
Top downloads: http://jap.aip.org/features/most_downloaded
Information for Authors: http://jap.aip.org/authors

ADVERTISEMENT

Downloaded 10 Jun 2013 to 143.248.103.214. This article is copyrighted as indicated in the abstract. Reuse of AIP content is subject to the terms at: http://jap.aip.org/about/rights_and_permissions

Electron-beam irradiation-induced gate oxide degradation

Byung Jin Cho,[a] Pei Fen Chong, and Eng Fong Chor
Department of Electrical and Computer Engineering, National University of Singapore, 10 Kent Ridge Crescent, Singapore 119260

Moon Sig Joo and In Seok Yeo
Hyundai Electronics Industries Company Limited, Memory R&D Division, Ichon-si, Kyungki-do 467-701, Korea

(Received 25 April 2000; accepted for publication 4 September 2000)

Gate oxide degradation induced by electron-beam irradiation has been studied. A large increase in the low-field excess leakage current was observed on irradiated oxides and this was very similar to electrical stress-induced leakage currents. Unlike conventional electrical stress-induced leakage currents, however, electron-beam induced leakage currents exhibit a power law relationship with fluency without any signs of saturation. It has also been found that the electron-beam neither accelerates nor initiates quasibreakdown of the ultrathin gate oxide. Therefore, the traps generated by electron-beam irradiation do not contribute to quasibreakdown, only to the leakage current.
© *2000 American Institute of Physics.* [S0021-8979(00)06923-1]

I. INTRODUCTION

Within the perspective of future device downscaling in modern complementary metal–oxide–semiconductor (CMOS) technologies, electron-beam (e-beam) lithography is considered to be one of the strong candidates as a next generation lithography tool,[1] in order to achieve the required fine geometry definition. However, e-beam irradiation onto a MOS structure can cause radiation-induced damage, especially to the thin gate oxide.[2] Thus, the study of gate oxide degradation induced by e-beam irradiation is imperative for the successful implementation of the future lithography tool. Radiation-induced degradation of MOS devices, based on observation of the flat band voltage shift (ΔV_{FB}) and interface trap densities (D_{IT}), has been reported to become less significant as the design rule of MOS field effect transistors (MOSFETs) shrinks and the gate oxide thickness becomes thinner.[3,4] However, low-field oxide leakage currents in thin gate oxides measured after irradiation,[5–7] indicated as radiation-induced leakage current (RILC), have recently been recognized as one of the hot topics of concern for the irradiated MOS device.[5–10] The RILC is similar to the well-known electrical stress-induced leakage current (SILC),[11–14] which is an important degradation phenomenon in thin gate oxides.[15,16] Besides the issues of low-field leakage current, quasibreakdown (QB), an anomalous degradation mode of ultrathin gate oxides has also attracted great attention[17–19] in recent years. Quasibreakdown, also known as soft breakdown, is usually identified by an abrupt increase of the leakage current at low gate field and a large fluctuation in the gate signal during constant current or voltage stress. Recent results of the quasibreakdown in ultrathin gate oxides have been presented,[20,21] but the mechanism of QB remains unanswered.

In this article, the nature of e-beam-induced gate oxide degradation is discussed. A comparative study of RILC with SILC will be addressed to clarify the behavior of RILC. The effect of e-beam on QB will then be discussed to better understand the long-term reliability of e-beam irradiated gate oxides.

II. EXPERIMENTAL PROCEDURE

For leakage current measurements and annealing experiments, test devices were n^+-polysilicon gate MOS capacitors with a 45 Å gate oxide, fabricated on *p*-type silicon wafers. The gate oxide was thermally grown in a pyrogenic ambient at 750 °C, followed by annealing in a N_2 ambient at 900 °C for 20 min. The area of the capacitors was 200 μm×200 μm for all measurements. The samples were irradiated by a Hitachi S2700 scanning electron microscope (SEM). In the experiments, the e-beam scans the entire gate area of every capacitor separately without photoresist in order to intentionally introduce damage into the gate oxides. The e-beam accelerating voltage used in this study was 25 kV. The e-beam irradiation dosage was controlled by varying the exposure time over a fixed scan area, which was equivalent to the area of a capacitor, at a fixed scan rate. Beam currents in the range of nA to μA were used to investigate the dependence of beam current on oxide degradation. During each irradiation of a sample, however, the beam current was kept constant. No bias was applied to the capacitors during irradiation. Gate current values were read after several repeated I_g–V_g sweep measurements in order to eliminate any transient components.[22,23]

Comparison with electrical SILC was made using samples stressed under a constant current density, ranging from −2 to −1000 mA/cm². For the experiments on QB, MOS capacitors with a 35 Å gate oxide were used. The occurrence of the QB phenomenon was monitored at the onset of gate voltage fluctuations during constant current stress (CCS). Once the gate voltage fluctuations began, the stress

[a]Electronic mail: elebjcho@nus.edu.sg

 © 2000 American Institute of Physics

Downloaded 10 Jun 2013 to 143.248.103.214. This article is copyrighted as indicated in the abstract. Reuse of AIP content is subject to the terms at: http://jap.aip.org/about/rights_and_permissions

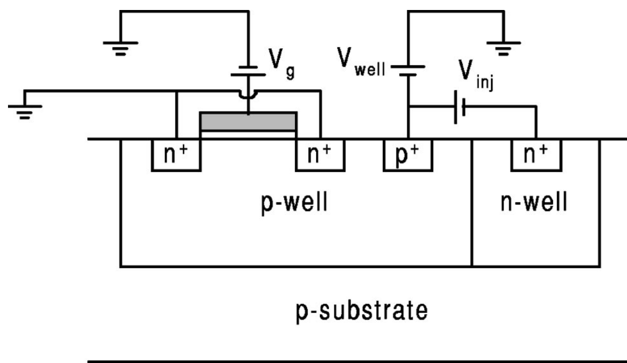

FIG. 1. Schematic drawing of the test structure and bias conditions for substrate hot electron injection. During hot electron injection, the gate voltage (V_g) was fixed at +3 V and the well voltage (V_{well}) was varied to control the energy of electrons injected into the oxide. The amount of substrate hot electron injection is controlled by a forward bias, V_{inj}, keeping a constant value of 3 V.

was stopped and the gate current–voltage characteristic was measured to confirm the occurrence of QB. This is necessary for the confirmation of the occurrence of QB.[17]

For the substrate hot electron injection (SHE) experiments,[24,25] n-channel n-MOSFETs, with a 45 Å gate oxide, fabricated using twin well and dual polysilicon gate technology, were used. The channel width and the length of the MOSFETs used in this experiment were 10 and 1 μm, respectively. A schematic drawing showing the test structure and bias conditions for substrate hot electron injection is depicted in Fig. 1. The gate voltage, V_g, was fixed at +3 V, while the source and the drain were grounded. The well voltage, V_{well}, was varied to control the energy of the hot electrons injected into the gate oxide during substrate hot electron injection. The adjacent n well was forward biased, and was used to control the amount of substrate hot electron injection. The forward-biased voltage was kept constant at +3 V during the experiment.

Thermal annealing of the MOS capacitors was performed in a N_2 ambient using a conventional horizontal tube furnace.

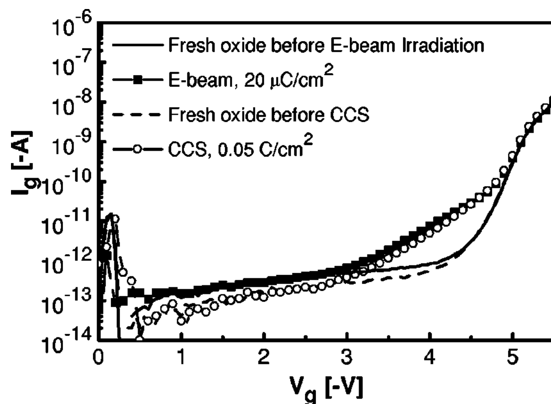

FIG. 2. I_g–V_g characteristics of fresh, e-beam irradiated (total dose of 20 μC/cm^2), and electrically stressed (total charge of 0.05 C/cm^2) oxides with a thickness of 45 Å. The current density used during constant current injection is -5 mA/cm^2. The small difference in the low-field regime is due to the sample-to-sample variation of the fresh samples.

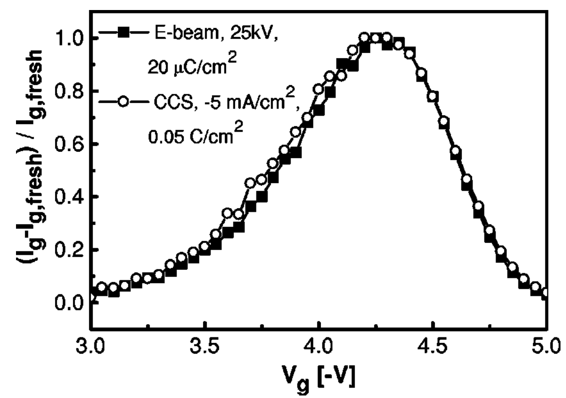

FIG. 3. Fractional excess leakage current, $(I_g - I_{g,\text{fresh}})/I_{g,\text{fresh}}$, for RILC and SILC for a 45 Å oxide. Both curves exhibit similar trends, peaking at about $V_g = -4.2$ V.

III. RESULTS AND DISCUSSIONS

A. Nature of RILC

Figure 2 shows the I_g–V_g characteristics of fresh, e-beam irradiated (total dose of 20 μC/cm^2), and electrically stressed (total charge of 0.05 C/cm^2) oxides with a thickness of 45 Å. Both the irradiation and the electrical stress exhibit significant excess leakage currents in the pretunneling regime and the curves for RILC and SILC resemble each other. The small difference in the low-field regime is due to the sample-to-sample variation of the fresh samples. The fractional excess leakage currents, defined in terms of $(I_g - I_{g,\text{fresh}})/I_{g,\text{fresh}}$, shown in Fig. 3, clearly demonstrate the similarity between the two currents. Both curves exhibit the maximum increment in the leakage current at about $V_g = -4.2$ V. Despite the fact that RILC and SILC show some similarities and are considered to have the same conduction mechanism, trap-assisted tunneling,[6,10] some differences are found in our experiment. Figure 4 shows a set of SILCs measured after stress with various charge fluency. The SILC increases with increasing stress charge injected, and gradually saturates above a certain amount of charge injected. After a certain degree of saturation, the current suddenly jumps to a very high value, which indicates the occurrence of QB. On the other hand, for RILC, the leakage current increases

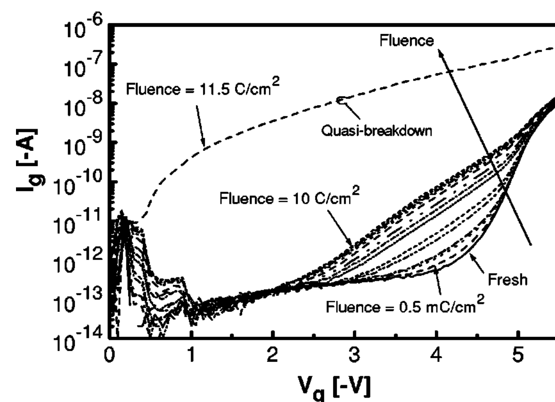

FIG. 4. SILCs of a 45 Å oxide measured after CCS using a constant current density of -5 mA/cm^2 with various charge fluencies.

Downloaded 10 Jun 2013 to 143.248.103.214. This article is copyrighted as indicated in the abstract. Reuse of AIP content is subject to the terms at: http://jap.aip.org/about/rights_and_permissions

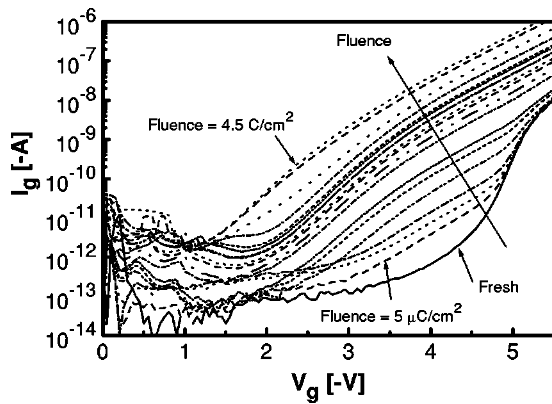

FIG. 5. RILCs of a 45 Å oxide measured after e-beam irradiation at an accelerating voltage of 25 kV with various e-beam dosages.

with increasing e-beam dosage, showing neither saturation nor a sudden jump of I_g–V_g characteristics, but gradually increasing up to the very high level of leakage current comparable to that of QB, as indicated in Fig. 5. Figure 6 shows the behavior of RILC and SILC more clearly. The excess leakage currents ΔI_g $[=(I_g-I_{g,\text{fresh}})]$ is plotted against stress charge fluency for both SILC and RILC with different stress current densities. The current values were read at V_g, corresponding to the peak fractional excess leakage currents in Fig. 3. It is observed that the gradients of ΔI_g versus charge fluence for the RILC and the initial stage of SILC are similar. This implies that the rate of generation of leakage current per unit charge injected for RILC and SILC is the same, suggesting that RILC and SILC may have a similar generation mechanism. The magnitude of RILC is also observed to be approximately two to three orders of magnitude higher than that of SILC for all stress current densities used in this work. Since it has been reported that both SILC and RILC are manifestations of a trap-assisted tunneling conduction mechanism across the oxide, mediated by neutral traps created during the electrical stress and e-beam irradiation,[6,10] the much higher value of RILC for the same fluency implies

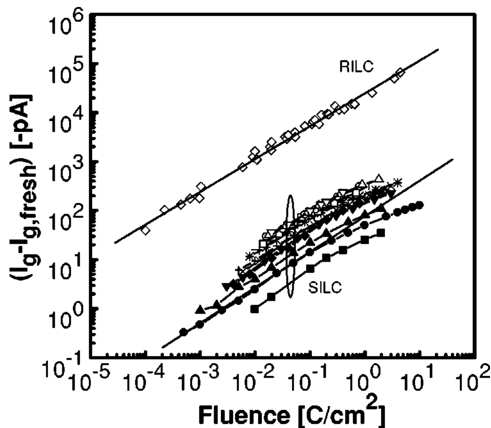

FIG. 6. Excess leakage current, $(I_g-I_{g,\text{fresh}})$, vs charge fluency for SILCs and RILCs. The current values were read at V_g corresponding to the peak point in Fig. 3. For SILC notations, ■: −2, ●: −5, ▲: −10, ▼: −30, ♦: −40, +: −50, ×: −60, ∗: −80, −: −100, |: −120, □: −140, ○: 160, △: −180, and ▽: −200 mA/cm². As for the RILC notation, ◇: e-beam, 25 kV.

that the e-beam generates a much larger number of neutral oxide traps compared to electrical stress. This means the trap generation probability is much higher under e-beam irradiation than under electrical stress, because of the much higher energy of incident electrons in e-beam irradiation.

As shown in Fig. 6, each data set for SILC shows two distinct regions. Initially, a power law relationship exists between ΔI_g and charge fluency for all stress current densities used. However, beyond a critical amount of charge injected, ΔI_g deviates from the power law and gradually saturates until the quasibreakdown or hard breakdown occurs. It is also seen that the magnitude of SILC for a given charge fluency is dependent on the stress current density. However, the starting point of SILC saturation is constant at about $\sim$0.2 C/cm² for a 45 Å thick gate oxide, even though the stress current density varies over two decades. On the other hand, the magnitude of RILC has no dependence on the electron beam current density during irradiation. (Note that the data points of RILC in Fig. 6 are obtained using various electron beam current densities ranging from nA to μA.) This implies that SILC dependence on current density may not be due to the difference in current density, but caused by the change in field and/or electron energy, as the stress current density and electric field vary concurrently in electrical stress. For RILC, it is observed that ΔI_g follows a power law relationship with the e-beam dosage throughout the entire range of dosage used. Neither saturation nor quasibreakdown is observed on any capacitor irradiated up to a dosage of $\sim$5 C/cm², the level at which most electrically stressed capacitors have already experienced quasibreakdown. The nonsaturation property of RILC strongly implies that the saturation of SILC is not due to the limited number of available empty traps that can carry the tunneling current as reported in the literature,[12] because the RILC, which has the same trap-assisted tunneling conduction mechanism as SILC, never saturates even though the magnitude is more than two orders higher than that of SILC. Since the differences between electrical stress and e-beam irradiation are the presence of electric field during stress or irradiation and the electron energy range, the saturation in SILC may be due to the presence of field or limited by the energy of electrons. During Fowler–Nordheim (FN) stress, the field and energy effects act upon the oxide concurrently. As shown in Fig. 7, as the electron energy increases with increasing oxide field, the excess leakage current is seen to saturate. Thus, it is necessary to separate the effects of electric field and electron energy on SILC saturation for better understanding of the nonsaturation property of RILC. Substrate hot electron injection experiments, therefore, were performed to investigate the effect of electron energy on the SILC characteristics, while the oxide field was kept constant. The energy of electrons injected into the oxide was controlled by varying V_{well} in Fig. 1 in the range from −8 to −14 V. Figure 8 shows the result of ΔI_g $[=I_g-I_{g,\text{fresh}})]$ versus charge fluency after SHE injection for various well voltages, with the gate voltage kept constant at 3 V. At this gate voltage, FN tunneling current is negligible, as can be noticed in Fig. 2. The result in Fig. 8 shows no saturation above a critical fluency. At large fluency, instead of saturation, as observed in FN injection, the increment rate of

Downloaded 10 Jun 2013 to 143.248.103.214. This article is copyrighted as indicated in the abstract. Reuse of AIP content is subject to the terms at: http://jap.aip.org/about/rights_and_permissions

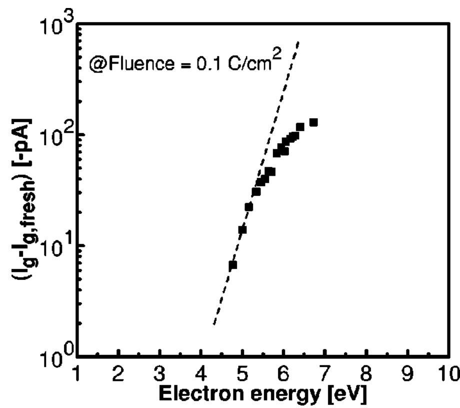

FIG. 7. Excess leakage current, (I_g–$I_{g,\mathrm{fresh}}$) vs energy of electrons for FN injections carried out at different constant current densities.

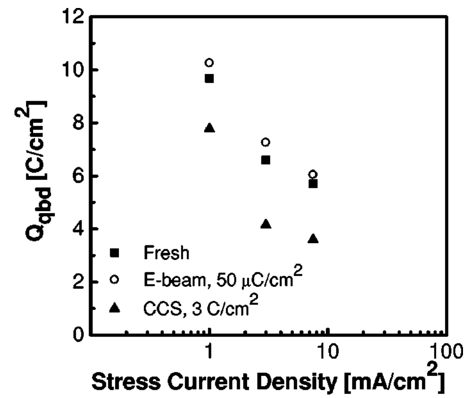

FIG. 9. Stress current density dependence of charge to quasi breakdown for fresh, electrically stressed, and e-beam irradiated oxides. No significant difference between irradiated and fresh oxides was found, implying that e-beam irradiation does not accelerate quasibreakdown.

ΔI_g increases with charge fluency. It is also observed that as the well potential increases, ΔI_g increases. This verifies that the increase of electron energy leads to a higher generation of traps which contribute to the trap-assisted tunneling. The result in Fig. 8 clearly shows that the saturation of ΔI_g does not happen at the low oxide field. As a consequence, since e-beam irradiation is done without any bias applied across the oxide, the nonsaturating behavior of RILC is attributed to the absence of an oxide field.

B. Effects on quasibreakdown

The quasibreakdown[17–21] characteristic after e-beam irradiation was also investigated for 35 Å gate oxides. CCS tests were performed on fresh oxides, pre-electrically stressed oxides (3 C/cm^2), and e-beam irradiated (50 μC/cm^2) oxides to evaluate the charge-to-quasibreakdown (Q_{qbd}). The amount of pre-electrical stress charge fluency and the radiation dose were selected such that the excess leakage currents were nearly the same for both conditions. Cumulative distributions of Q_{qbd} values were first obtained for three different stress current densities. Subsequently, the 50th percentile point of each cumulative failure plot of the Q_{qbd} distribution was used to obtain the Q_{qbd} dependence on stress current density. Each data point in Fig. 9 was obtained from over 30 samples. The result in Fig. 9 shows that e-beam irradiation does not lead to any change in Q_{qbd} relative to the fresh oxides, despite the increase in leakage current after e-beam irradiation. However, the Q_{qbd} of prestressed CCS samples is shifted by as much as 3 C/cm^2, as expected. Therefore, it can be concluded that e-beam irradiation does not accelerate quasibreakdown of ultrathin gate oxides.

In Fig. 6, it is seen that e-beam does not initiate QB up to a dosage of $\sim$5 C/cm^2, at the level which most electrically stressed capacitors have already experienced quasibreakdown or even hard breakdown. Hence, it is suggested that e-beam neither accelerates nor initiates QB. This is probably due to the absence of an oxide field during irradiation. In the absence of field, high-energy electrons are injected uniformly across the oxide, corresponding to a symmetrical distribution of neutral defects across the oxide.[6] By comparing the magnitude of RILC at high e-beam dosages (Fig. 5) to the leakage current level of QB (Fig. 4), one would agree that the oxide irradiated with a high e-beam dose has a comparable amount of traps to the oxide experienced QB since their leakage current levels are comparable. However, the fact that e-beam does not accelerate or initiate QB leads us to conclude that the traps generated by e-beam irradiation do not contribute to QB, only to RILC.

One might argue that oxides irradiated with high e-beam dosages have actually experienced QB because their leakage

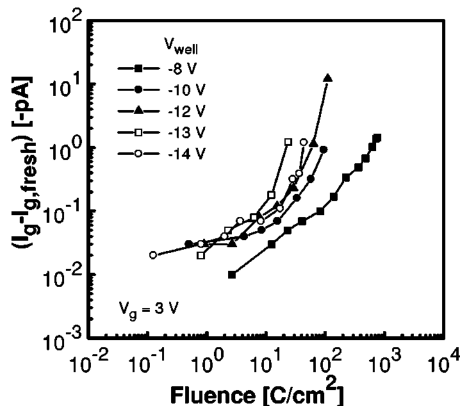

FIG. 8. Excess leakage current, (I_g–$I_{g,\mathrm{fresh}}$) vs fluency after substrate hot electron injection for various well voltages. The gate voltage was constant at 3 V.

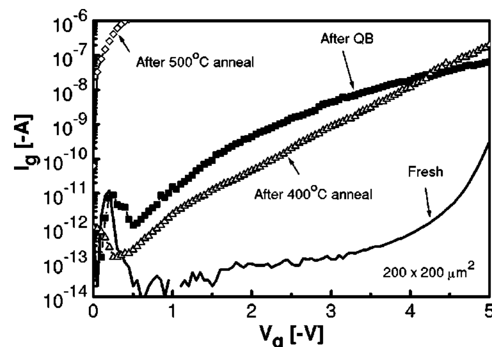

FIG. 10. I_g–V_g characteristics of fresh oxide and of oxides after quasibreakdown and with annealing in a N_2 ambient for 10 min at 400 and 500 °C.

Downloaded 10 Jun 2013 to 143.248.103.214. This article is copyrighted as indicated in the abstract. Reuse of AIP content is subject to the terms at: http://jap.aip.org/about/rights_and_permissions

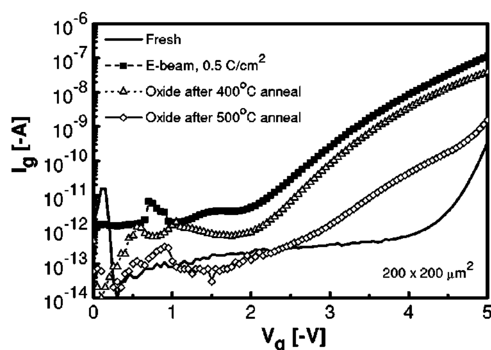

FIG. 11. I_g–V_g characteristics of fresh oxide and of oxides after e-beam irradiation and with annealing in a N_2 ambient for 10 min at 400 and 500 °C.

current levels are comparable to those of QB. To verify that they are in two different statuses, a series of annealing experiments were conducted. The oxides experiencing QB by electrical stress were annealed in a N_2 ambient at 400 or 500 °C for 10 min. After a 400 °C anneal, the leakage current decreases at low field, but increases at high field, as shown in Fig. 10. After a 500 °C anneal, the oxide undergoes complete breakdown. This is a typical annealing characteristic of oxides with QB and details of this will be published elsewhere.[26] On the other hand, for oxides irradiated with a dosage of ~0.5 C/cm^2, thermal annealing always decreases the RILC and higher temperature annealing is always more effective in the reduction of RILC, as illustrated in Fig. 11. This is attributed to the annealing of oxide traps which contribute to RILC. This different annealing behavior confirms that the RILC and the leakage current after QB have two different mechanisms.

IV. CONCLUSIONS

Gate oxide degradation induced by e-beam irradiation has been studied in this work based on a comparison with electrical stress-induced degradation. Despite having the same conduction mechanism, RILC and SILC exhibit some differences. RILC is shown to exhibit a power law relationship with fluency without any signs of saturation, which deviates from that observed in the conventional SILC fluency dependence. This discrepancy is believed to be due to the absence of an oxide field during e-beam irradiation. This is supported by the substrate hot electron injection experimental results, indicating that SILC also never saturates at a low oxide field. With a high energy of electrons of ~25 keV, the RILC current level is observed to be almost approximately two to three orders of magnitude higher than that of SILC. Since both SILC and RILC have the same conduction mechanism, this can be accounted for by the high energy of electrons during e-beam irradiation relative to that during FN injection. These results also show that the saturation region in SILC is not caused by the limited number of available empty traps that can carry the tunneling current, as reported previously.

In the case of quasibreakdown, the results showed that e-beam neither accelerates nor initiates QB. This phenomenon has been attributed to the absence of an oxide field during e-beam irradiation. The very high leakage current level without the occurrence of QB after a high dose e-beam irradiation strongly implies that the traps generated by e-beam irradiation do not contribute to QB.

[1] P. Castrucci, W. Henley, and W. Liebmann, Solid State Technol. **40**, 127 (1997).
[2] T. P. Ma and P. V. Dressendorfer, *Ionizing Radiation Effects in MOS Devices and Circuits* (Wiley, New York, 1989), p. 87.
[3] A. B. Joshi and D.L. Kwong, Electron. Lett. **28**, 744 (1992).
[4] A. J. Lelis and T. R. Oldham, IEEE Trans. Nucl. Sci. **40**, 1367 (1993).
[5] A. Scarpa, A. Paccagnella, F. Montera, G. Ghibaudo, G. Pananakakis, G. Ghidini, and P. G. Fuochi, IEEE Trans. Nucl. Sci. **44**, 1818 (1997).
[6] M. Ceschia, A. Paccagnella, A. Cester, A. Scarpa, and G. Ghidini, IEEE Trans. Nucl. Sci. **45**, 2375 (1998).
[7] P. F. Chong, B. J. Cho, E. F. Chor, M. S. Joo, and I. S. Yeo, Extended Abstracts of the 1999 International Conference on Solid State Devices and Materials, The Japan Society of Applied Physics, Tokyo, p. 182.
[8] A. Scarpa, A. Paccagnella, F. Montera, A. Candelori, G. Ghibaudo, G. Pananakakis, G. Ghidini, and P. G. Fuochi, IEEE Trans. Nucl. Sci. **45**, 1390 (1998).
[9] A. Candelori, A. Paccagnella, M. Cammarata, G. Ghidini, and P. G. Fuochi, IEEE Trans. Nucl. Sci. **45**, 2383 (1998).
[10] B. J. Cho, S. J. Kim, C. H. Ling, M. S. Joo, and I. S. Yeo, Proceedings of the 7th International Symposium on the Physical and Failure Analysis of Integrated Circuits, IEEE, Singapore, 1999, p. 30.
[11] R. Rofan and C. Hu, IEEE Electron Device Lett. **12**, 632 (1991).
[12] D. J. DiMaria and E. Cartier, J. Appl. Phys. **78**, 3883 (1995).
[13] E. F. Runnion, S. M. Gladstone, R. S. Scott, D. J. Dumin, L. Lie, and J. C. Mitros, IEEE Trans. Electron Devices **44**, 993 (1997).
[14] K. Sakakibara, N. Ajika, M. Hatanaka, H. Miyoshi, and A. Yasuoka, IEEE Trans. Electron Devices **44**, 986 (1997).
[15] P. Olivo, T. N. Nguyen, and B. Ricco, IEEE Trans. Electron Devices **35**, 2259 (1988).
[16] R. Degraeve, B. Kaczer, and G. Groeseneken, Microelectron. Reliab. **39**, 1445 (1999).
[17] S. H. Lee, B. J. Cho, J. C. Kim, and S. H. Choi, Tech. Dig. Int. Electron Devices Meet. IEEE, 605 (1994).
[18] M. Depas, T. Nigam, and M. M. Heyns, IEEE Trans. Electron Devices **43**, 1499 (1996).
[19] F. Crupi, R. Degraeve, G. Groeseneken, T. Nigam, and H. E. Maes, IEEE Trans. Electron Devices **45**, 2329 (1998).
[20] H. Guan, B. J. Cho, M. F. Li, Y. D. He, Z. Xu, and Z. Dong, in Ref. 10, p. 81.
[21] J. H. Stathis, J. Appl. Phys. **86**, 5757 (1999).
[22] K. Sakakibara, N. Ajika, M. Hatanaka and H. Miyoshi, Proceedings of the 34th International Reliability Physics Symposium, IEEE, Dallas, 1996, p. 100.
[23] R. S. Scott and D. J. Dumin, IEEE Trans. Electron Devices **43**, 130 (1996).
[24] D. J. DiMaria, J. Appl. Phys. **86**, 2100 (1999).
[25] B. J. Cho, Z. Xu, H. Guan, and M. F. Li, J. Appl. Phys. **86**, 6590 (1999).
[26] Z. Xu, B. J. Cho, and M. F. Li, Microelectron. Reliab. **40**, 1341 (2000).

Downloaded 10 Jun 2013 to 143.248.103.214. This article is copyrighted as indicated in the abstract. Reuse of AIP content is subject to the terms at: http://jap.aip.org/about/rights_and_permissions